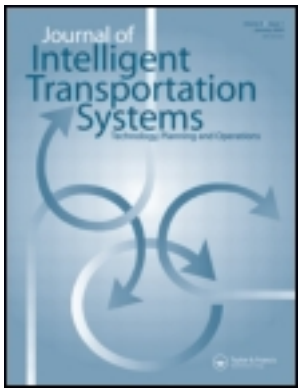

Journal of Intelligent Transportation Systems: Technology, Planning, and Operations
Publication details, including instructions for authors and subscription information:
http://www.tandfonline.com/loi/gits20

An Exploratory Shockwave Approach to Estimating Queue Length Using Probe Trajectories

Yang Cheng [a], Xiao Qin [b], Jing Jin [c] & Bin Ran [a d]

[a] Department of Civil and Environmental Engineering, University of Wisconsin-Madison, Madison, Wisconsin, USA

[b] Department of Civil and Environmental Engineering, South Dakota State University, Brookings, South Dakota, USA

[c] Center for Transportation Research, University of Texas at Austin, Austin, Texas, USA

[d] School of Transportation, Southeast University, Nanjing, China

Accepted author version posted online: 21 Nov 2011.Version of record first published: 01 Feb 2012.

To cite this article: Yang Cheng , Xiao Qin , Jing Jin & Bin Ran (2012): An Exploratory Shockwave Approach to Estimating Queue Length Using Probe Trajectories, Journal of Intelligent Transportation Systems: Technology, Planning, and Operations, 16:1, 12-23

To link to this article: http://dx.doi.org/10.1080/15472450.2012.639637

Journal of Intelligent Transportation Systems, 16(1):12–23, 2012

ISSN: 1547-2450 print / 1547-2442 online
DOI: 10.1080/15472450.2012.639637

Taylor & Francis
Taylor & Francis Group

An Exploratory Shockwave Approach to Estimating Queue Length Using Probe Trajectories

YANG CHENG,[1] XIAO QIN,[2] JING JIN,[3] and BIN RAN[1,4]

[1]Department of Civil and Environmental Engineering, University of Wisconsin–Madison, Madison, Wisconsin, USA
[2]Department of Civil and Environmental Engineering, South Dakota State University, Brookings, South Dakota, USA
[3]Center for Transportation Research, University of Texas at Austin, Austin, Texas, USA
[4]School of Transportation, Southeast University, Nanjing, China

In this article, the authors present an innovative approach for signalized intersection performance measurement using probe vehicle trajectory data, focusing on queue length estimation. Critical points, defined as the data points representing the changes in vehicle dynamics, are the keystone of the methodology. The author then present a threshold-based critical point extraction algorithm, which has the potential to reduce the communication cost in future real-time probe data collection application. A shockwave-based method using the critical points to detect the signal timing provides the basis for cycle-by-cycle performance measurement. The authors propose a queue length estimation method as a case study for signalized intersections. This approach was tested by simulation and Next Generation Simulation Project data. Results indicate promising outcome of the trajectory-based method.

Keywords Signalized Intersection; Probe Trajectory; Queue Length Estimation; Signal Detection

INTRODUCTION

Arterial performance measurements are essential for advanced traffic management systems and advanced traveler information systems. Although nearly 40% of the nation's vehicle-miles traveled occurs on arterials, real-time arterial performance measurement systems are not as mature as their freeway counterparts. Two of the biggest challenges are (a) arterial traffic conditions are more complicated than the ones on freeways because of the periodic interruptions from traffic signals, random friction from crossing traffic on minor streets, and so forth; and (b) current traffic data collection systems deployed on arterials are insufficient for measuring real-time operational performance (Balke, Charara, & Parker, 2005).

Given these challenges, recent research development is focused on providing real-time performance measure, including (a) investigating the relation between performance measures and traffic/control conditions and (b) developing new data collection technologies and data sources. For example, in the first area, an analytical travel-time estimation model (Skabardonis & Geroliminis, 2008) uses inductive loop detector data (aggregated in 20 or 30 s) and signal timing as the model input. The model carefully calculates the delay as the sum of signal delay, queuing delay, and oversaturation delay. By the same token, other work uses stochastic theories (Geroliminis & Skabardonis, 2005; Viti & van Zuylen, 2009) or artificial intelligence methods (Cheu, Lee, & Xie, 2001; Robinson & Polak, 2005). Growing interests in the second area develop along with the emerging and advancement of traffic probe technologies; new data sources and high-resolution data become available, such as individual vehicle arrival data from advanced signal control devices (Balke et al., 2005; Liu, Ma, Wu, & Hu, 2008), vehicle reidentification data (Coifman, 2002; Liu, Oh, Oh, Chu, & Recker, 2001; Ritchie, Jeng, Tok, & Park, 2008; Wilson, 2008), and probe data (Ahmed, El-Darieby, Abdulhai, & Morgan, 2008; Ban, Herring, Hao, & Bayen, 2009; Fontaine & Smith, 2007; Pan, Lu, Wang, & Ran, 2007; Qiu & Ran, 2008).

The paper was partly supported by the National High Technology Research and Development (863) Program of China (Grant No. 2011AA110404 and 2011AA110405).

Address correspondence to Yang Cheng, University of Wisconsin–Madison, 1206 Engineering Hall, 1415 Engineering Drive, Madison, WI 53706. E-mail: cheng8@wisc.edu

The development of traffic detection technologies makes the use of probe vehicle trajectory data possible. There are some studies about using trajectories of all vehicles for shockwave detection (Izadpanah, Hellinga, & Fu, 2009; Lu & Skabardonis, 2007). There are also a few attempts of using vehicle trajectories for performance measurement (Berkow, Monsere, Koonce, Bertini, & Wolfe, 2009; Claudel, Hofleitner, Mignerey, & Bayen, 2009). The detailed trajectory data can provide more abundant and detailed traffic information than can travel time of a predefined route, especially for arterials. Congestion can be easily detected using trajectory data because trajectories can directly reveal low speeds and frequent stops. In contrast, the number of available sampled travel times would drastically decrease at low flow rate because probe travel times will only be available after the probe vehicle finishes the prespecified route. The main challenge of developing a trajectory-based model is how to convert the microscopic detection into macroscopic performance measurement. One trajectory only represents individual behavior of a vehicle, which is subject to actual situations encountered by the driver. Therefore, the probe trajectory data are more volatile. In a freeway travel-time estimation model (Claudel et al., 2009), the probe trajectories are converted to density estimation using the Moskowitz function (Daganzo, 2005; Newell, 1993). The arterial situations are more complicated because of the periodic turbulence caused by signals and local frictions. Comert and Cetin (2007) studied the conditional probability distribution of the queue length at an isolated intersection, given the probe vehicle locations in the queue. They found that only the location of the last probe in the queue is necessary for queue length estimation. However, the assumption of knowing the actual percentage of probe vehicles in the traffic stream limits its application.

The existing work related to arterial trajectory data has not really led to practical applications of providing real-time information. This article explores the feasibility of using vehicle trajectory data for signalized intersection performance measurement, choosing cycle-by-cycle queue length estimation as the start point. The proposed approach defines the trajectory's critical points (CPs), which are able to capture the dynamics of the vehicular movement in a space-time diagram. A method was developed to extract the CPs and shockwave-based methods were used to detect signal timing and to estimate the cycle-by-cycle queue length. The theories were tested by numeric experiment using simulation data and real trajectory data from Next Generation SIMulation (NGSIM) Project (Alexiadis, Colyar, & Halkias, 2004).

METHODOLOGY

Given the intersection and link geometric characteristics, the intent is to develop a real-time intersection performance model using vehicle trajectory data as the only input. Figure 1 shows the overall building blocks for the methodology and the relation between them. The *critical point extraction* module reduces the trajectories to a series of CPs. The *critical points filter* module selects three types of CPs for different purposes. The signal timing is detected and the queue length in a cycle is estimated.

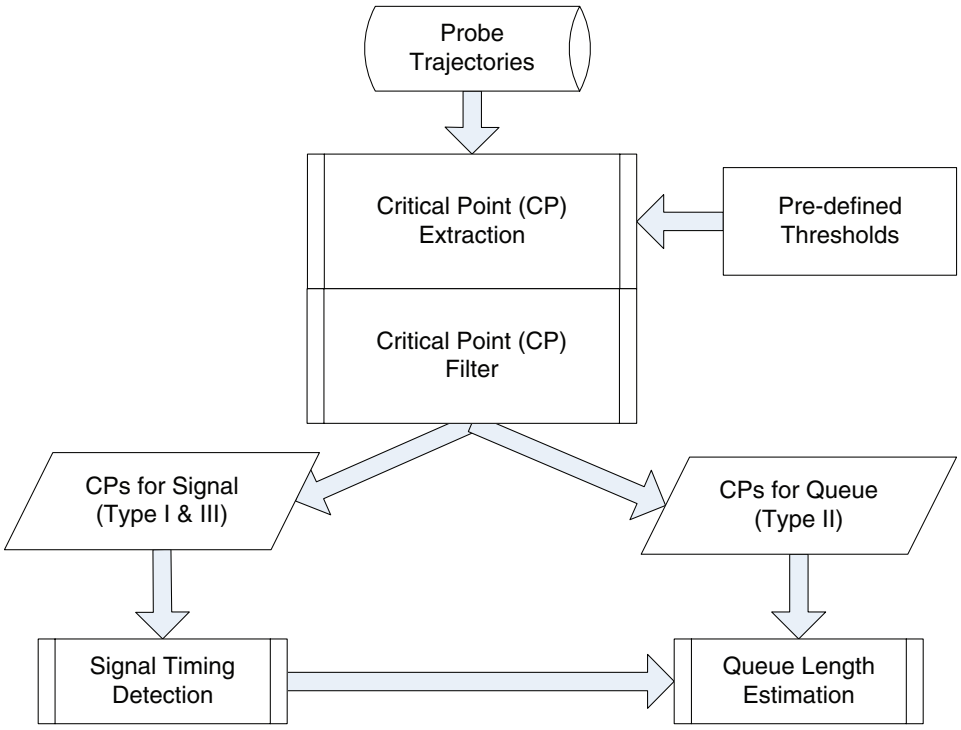

Figure 1 Methodology flow chart (color figure available online).

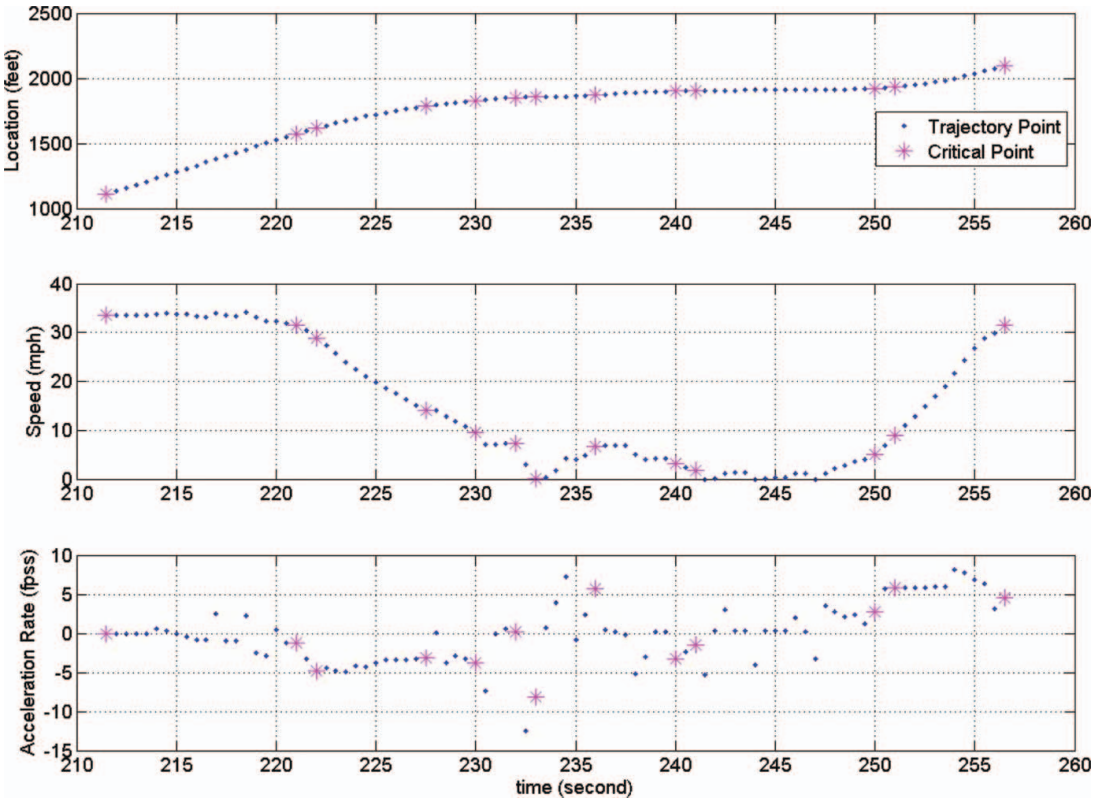

Figure 2 Critical points at a trajectory (Paramics simulation data) (color figure available online).

Modeling Trajectories

The trajectory of a vehicle can be described as a series of points, $\{x_t\}$, where x_t is a record of the vehicle at time t. x_t is a vector that describes the dynamics of vehicle at time t; $x_t = [l, v, a]$, where l is the location, v is the speed and a is the acceleration rate. l, v and $a$represent the three dynamic features.

The movement of a vehicle is not completely random. Drivers can be assumed rational as they fulfill three major tasks: (a) maintaining a desired speed, (b) keeping a safe distance from the lead vehicle, and (c) following the signal indication. In a general case, the trajectory of a vehicle can be divided into several regimes, which are either uniform motion or uniformly acceleration motion. CPs, $\{x_t^c\}$, a subset of $\{x_t\}$, are places where the movement regime changes. Therefore, the trajectory $\{x_t\}$ can be simplified to a set of CPs as shown in Figure 2.

($c_v = 3mph$, $c_a = 3fpss$, $c_{v,stop} = 3mph$; see next section)

The vehicles are assumed to travel on a one-dimensional road. Although the situations of lane changing or overtaking behavior are not explicitly discussed in this study, the one-dimensional assumption can be extended to two-dimensional by defining the lane as the fourth dynamic feature besides location, speed and acceleration rate.

From the information science perspective, the trajectories can be treated as a signal series. Converting $\{x_t\}$ to $\{x_t^c\}$ is analogous to data reduction, which benefits the real-time probe data collection by reducing the volume of data transmitted. If the onboard device operates a CP extraction program, only real-time CP data will be uploaded and communication cost will be reduced. It is obvious that this approach has the advantage over the current probe measurement technologies, which record at a fixed time interval.

Critical Points Extraction

The trajectory between two CPs is definitive and belongs to one of the two basic movements: (a) uniform motion (including stopping as a special case), and (b) uniformly acceleration motion (including deceleration). Therefore, a trajectory can be divided into several regimes with CPs as the boundaries; each regime belongs to one of the two basic movements.

Within each regime, either Eq. (1) or (2) is satisfied:

$$\text{if } |a_i| < c_a,$$
$$|\tilde{v} - v_i| < c_v \tag{1}$$
$$\text{if } |a_i| \geq c_a,$$
$$|\tilde{a} - a_i| < c_a \tag{2}$$

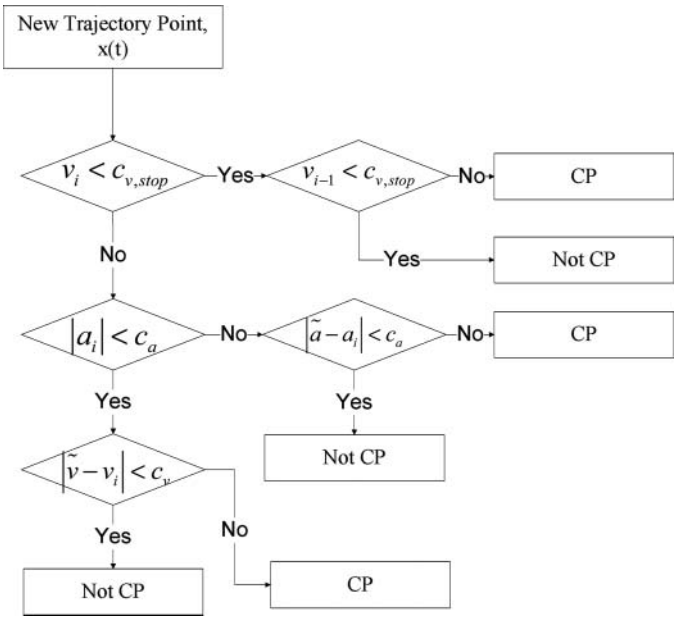

Figure 3 Critical points extraction algorithm logic.

where,

$\tilde{v}$ is the median speed of $\{x_i\}, i = 1, 2 \ldots n$;

c_v is a speed threshold;

$\tilde{a}$ is the median acceleration rate of $\{x_i\}, i = 1, 2 \ldots n$; and

c_a is an acceleration rate threshold.

Eq. (1) represents the uniform motion and Eq. (2) represents uniformly accelerated motion. In addition, considering the end of queue detection, it is necessary to treat stopping or very low speed as a special case; otherwise, the actual point when and where the vehicle joins the standing queue might be missed. A new speed threshold $c_{v,stop}$ is introduced. When Eq. (1) is satisfied (i.e., the regime is in a uniform motion), if Eq. (3) is satisfied, it is a stopping regime:

$$v_i < c_{v,stop} \tag{3}$$

The logic of the CP extraction algorithm is shown in Figure 3. After a CP is extracted, the trajectory before this CP is discarded and this CP becomes the first point of the rest of trajectory.

The calibration efforts would be moderate for these thresholds. According to the definition of CPs, the values of these thresholds are directly related to the acceleration and deceleration characteristics of vehicles, instead of traffic conditions or geometrics. CPs subscribe the changes in vehicle kinematics. The speed and acceleration rate thresholds are used to define to what extent the difference of any two consecutive segments on a trajectory is large enough to be considered as two different motions; the stopping speed threshold is for determining stopping. The *Travel Time Data Collection Handbook* (Turner, Eisele, Benz, & Holdener, 1998, p. 5) suggests that "typically" less than 5 mph be considered as stopping. It was found that the lower threshold can locate the point when the vehicle joins the standing queue more accurately. The selection of the thresholds can be determined by the user. According to the experiment, it is suggested that c_v be no larger than 6 mph, c_a be no larger than 5 fpss and $c_{v,stop}$ be less than 5 mph. In the "Numerical Experiment" section, $c_v = 3\ mph$, $c_a = 3 fpss$ and $c_{v,stop} = 3\ mph$ were used.

In comparison with several previous studies in identifying and analyzing shockwaves using vehicle trajectories (Izadpanah et al., 2009; Lu & Skabardonis, 2007), the CP defined in this article is different in the assumption, algorithm, and application:

1. Assumptions are different

   The CP in this article is used to extract the movement change at the trajectory while "joint point" (Izadpanah et al., 2009, p. 2) and "local minima" (Lu & Skabardonis, 2007, p. 3) are for detecting "major shockwaves." The *joint point* stands for the connecting point of trajectory segments, assuming the trajectory consists of segments of uniform movements; whereas the *local minima* means the points of speed drop. It can almost be certain that for arterials, the joint points are a subset of the CPs for the same trajectory. The CP is for a sampled probe approach, whereas local minima and joint points are not.

2. Extraction algorithms are different

   Given the different assumptions, the CP extraction algorithm proposed in this article is simple for real-time implementation with lower computational cost. The local minima method searches the local minimal speed points within a time window, and the joint point method uses an iterative two-phase piecewise regression model for the location domain. Although generated CPs tend to have more noise, establishing proper thresholds and a well-designed "selection of critical points" module can reduce noise significantly.

3. Potential applications are different

   Our algorithm can be used in the onboard GPS device to reduce the communication cost. In addition, CPs may include useful details about how the speed changes, which are valuable for other research such as vehicle emission and traffic safety.

Critical Points Filter for Various Purposes

Because of the changes in vehicle dynamics, the extracted CPs are different, which can be used for various purposes. A filter should be applied to choose the appropriate CPs. For example, when CPs are used for signal detection, only the CPs that result from signal changes should be used.

Figure 4 demonstrates three types of CPs: Type I is defined as the CP at the beginning point of a deceleration regime caused by signal light turning to red; Type II is defined as the CP at the point when the vehicle slows down and joins the queue; Type III is defined as the CP at the beginning point of an acceleration regime caused by signal light turning to green.

The three types of CPs need to be distinguished from the CPs related to small traffic flow disturbances and other irrelevant factors. We propose a filtering algorithm on the basis of these features of CPs: (a) time difference and (b) speed difference. The algorithm can be described as follows:

- Order all of the CPs from this vehicle chronologically and find the minimum speed CPs (index $j_1, j_2 \ldots j_m$) with speeds less than $c_{v,stop}$; if no such CP exist, this vehicle is not stopped by a standing queue, and Type II and Type III CPs do not exist in the current trajectory.
- Let $p = j_1$, find the first CP whose speed is less than its immediate previous CP with index of i; if the speed of CP i is higher than all the CPs from i to j, i is the Type I CP and go to (c); if not, throw away the CP from first to i, do this step again;
- CP j_m is the Type II CP; CP $j_m + 1$ is the Type III CP.

Figure 5 shows the selected Type I, II, and III CPs from the generated CPs.

Signal Timing Detection

Traffic signals are the major factor which affecting the traffic on arterials. However, real-time signal timing is not always available for online or even offline operations. According to the *2007 National Traffic Signal Report Card Technical Report* (National Transportation Operations Coalition, 2007, p. 19), "traffic monitoring and data collection" received a score of F and "almost half of agencies (43 percent) reported having little to no regular, ongoing program for collecting and analyzing traffic data for signal timing." Ban et al. (2009) explored the methods to derive signal timing using the delay measurement by virtual trip line technology based on GPS-equipped cell phones. Using sampled travel times, they found that a 40% penetration rate of probe was needed to obtain reliable signal timing detection. Using trajectory data can help detect signal timing data with a lower sample rate. It is known that vehicle movement changes are caused by the formation and dissipation of the queue before a traffic signal. In addition, the movement changes of a vehicle are actually captured by CPs. Hence, the signal timing parameters such as cycle length and green time can be obtained.

The fundamental and most widely used traffic flow model is the Lighthill-Whitham-Richards model (Lighthill & Whitham, 1955a, 1955b; Richards, 1956). The solution of this model is based on the conservation equation of the traffic flow and a function of speed, flow (or density). The propagation speed of a shockwave is calculated as follows:

$$v = \frac{q_u - q_d}{k_u - k_d} \tag{4}$$

where q_u, q_d are the flow rate for upstream and downstream, respectively, and k_u, k_d are the density for upstream and downstream, respectively.

As demonstrated in Figure 4 and 5, since the location and time of CPs are known from the trajectories, the start times of green and red can be determined once the shockwave speeds are estimated.

After the start of green, the queue begins to discharge. The start time of the green can be calculated as follows:

$$T_g = T^*_{CP3} - \frac{L^*_{CP3}}{v_{dis}} \tag{5}$$

T^*_{CP3} is the adjusted time stamp of the Type III CP. $T^*_{CP3} = T_{CP3} - v_{CP3}/a_{CP3}$, where T_{CP3} is the time stamp of the Type III CP, and v_{CP3}, a_{CP3} are the speed and acceleration rate of this Type III CP. L^*_{CP3} is the adjusted distance from the Type III CP to the stop bar. $L^*_{CP3} = L_{CP3} + v^2_{CP3}/2a_{CP3}$, where L_{CP3} is the distance from the Type III CP to the stop bar. The adjusted time and distance are used to compensate the detection errors by the CP extraction algorithm. v_{dis} is the queue discharge shockwave speed.

At the beginning of a green light, assume there is no queue spillback at the downstream intersection, the queue discharges at the saturation flow rate. The queue discharge shockwave speed can be estimated as follows:

$$v_{dis} = \frac{q_s - 0}{k_m - k_j} \tag{6}$$

where q_s is the saturation flow rate, k_m is the saturation flow density, and k_j is the jam density. In the "Numerical Experiment" section, $v_{dis} = 15\ mph$ was used.

After the start of red, traffic is stopped before the stop bar and a queue is formed. The start time of the red can be obtained by the following equation:

$$T_r = T^*_{CP1} - \frac{L^*_{CP1}}{v_{form}} \tag{7}$$

T^*_{CP1} is the adjusted time stamp of the Type I CP. $T^*_{CP1} = T_{CP1} - c_v/|a_{CP1}|$, where T_{CP1} is the time stamp of the Type I CP, and a_{CP1} are the speed and acceleration rate of this Type I CP. L^*_{CP1} is adjusted distance from the Type I CP to stop bar. $L^*_{CP1} = L_{CP1} + (2v_{CP1} + c_v)c_v/2\,|a_{CP1}|$, where v_{CP1} is the speed of the Type I CP and L_{CP1} is the distance from the Type I CP to the stop bar. v_{form} is the queue formation shockwave speed.

The queue formation shockwave can be estimated as follows:

$$v_{form} = \frac{0 - q_u}{k_j - k_u} \tag{8}$$

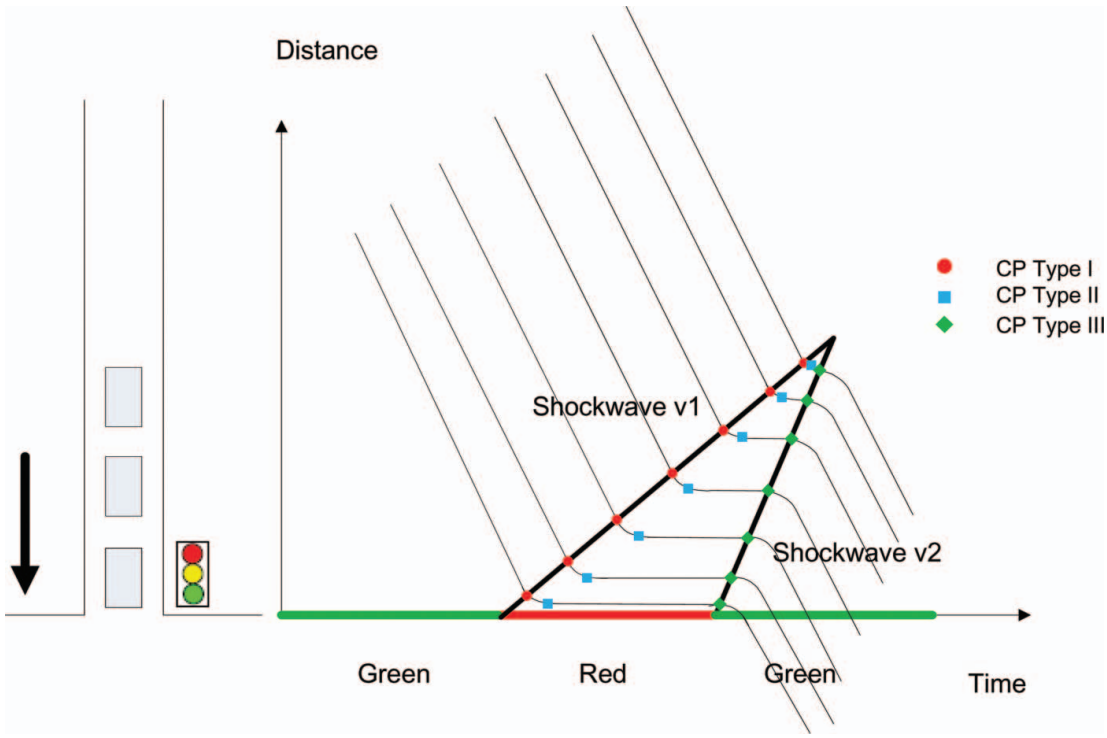

Figure 4 Shockwaves and critical points (CPs) (color figure available online).

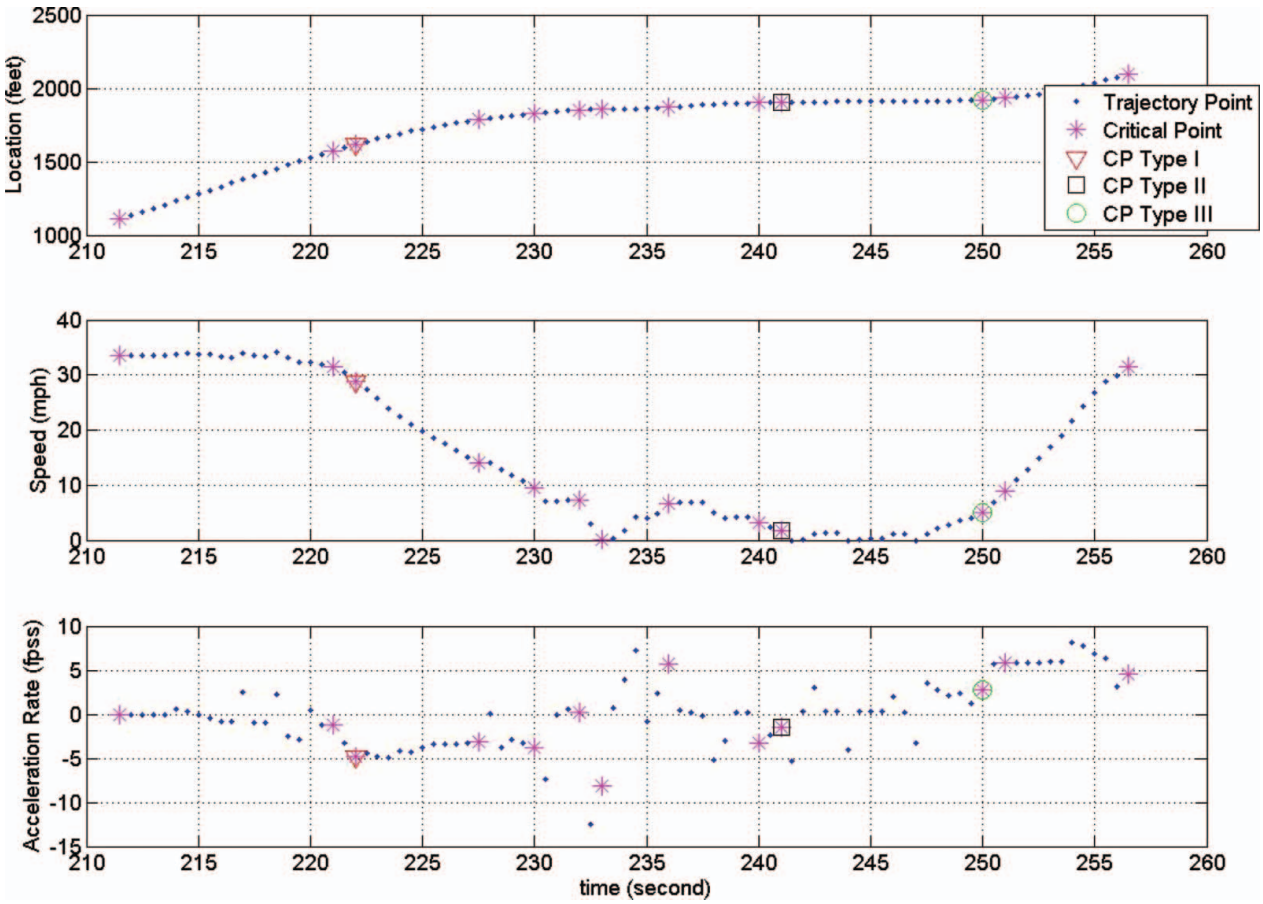

Figure 5 Critical points (CPs) and the selected CPs for further applications at a trajectory (Paramics simulation data) (color figure available online).

where q_u is the upstream arrival flow rate, k_u is the upstream arrival density, and k_j is the jam density.

The problem is now getting q_u and k_u. Using the basic flow-speed-density relationship $q = kv$, either q_u or k_u can be determined by the other because the inflow speed can be estimated by the vehicle speed before deceleration. There is no direct way to estimate q_u or k_u, but the average density $\overline{k_{CP1}}$ in terms of the number of vehicles between the stop bar and a Type I CP can be estimated without considering lane changing activities:

$$\overline{k_{CP1}} = \frac{L_{CP2}}{L_{CP1}} k_j \tag{9}$$

where L_{CP2} is the distance between the Type II CP and the stop bar.

Therefore, Eq. (8) is rewritten and approximated as follows:

$$v_{form} = \frac{0 - q_u}{k_j - \overline{k_{CP1}}} = -\frac{q_u/\overline{k_{CP1}}}{k_j/\overline{k_{CP1}} - 1} \approx -\frac{v_{CP1}}{L_{CP1}/L_{CP2} - 1} \tag{10}$$

where v_{CP1} is the speed of the Type I CP.

Dynamic Queue Length Estimation

Type II CPs correspond to the time and location when the vehicle joins the end of the queue. They can be used to detect the instantaneous queue length, or the end of the queue.

The progress of the queue formation and dissipation is greatly affected by the arrival pattern. For an isolated intersection, the arrival flow rate within a cycle can be assumed to be constant. Therefore, the incremental queue length can be calculated using the detected end of queue. Given the detected signal timing, the maximum queue length can be calculated as follows:

$$L_q = \frac{q_s q_u (T_g - T_r)}{k_j (q_s - q_u)} \tag{11}$$

The upstream arrival rate $q_u$can be estimated as follows:

$$q_u = \frac{L_{CP2}}{k_j (T_{CP2} - T_r)} \tag{12}$$

where L_{CP2} is the distance between the Type II CP and the stop bar, and T_{CP2} is the timestamp of the Type II CP.

Eq. (11) is used for cases without an initial queue. Considering there are stopped vehicles from the previous cycle, initial queue should be detected first and then the total queue length can be estimated. The following formula can help to detect initial queues:

$$q_s (T_{CP2} - T_r) < L_{CP2} k_j \tag{13}$$

If Eq. (13) satisfies, the initial queue exists and the length of the initial queue can be estimated by the following:

$$L_{q0} = L_{CP2} - (T_{CP2} - T_r) q_s / k_j \tag{14}$$

For an intersection affected by an upstream signal such as coordination, the arrival pattern varies within a cycle because of the gating effect. The flow pattern from upstream crossing streets may be significantly different from the main direction. The resulting queue formation process is a complex process. As an approximation, the queue increase process can be modeled as a piecewise linear line (Figure 6). More than one Type II CP is needed for this case. Assume there are $n - 1$ available Type II CPs, plus the point of the start of red (with the zero distance to the stop bar), and order them chronologically as a series of points on the queue length and time plane. Now, the average queue increase rate between each two consecutive points can be calculated as follows:

$$r_i = \frac{L_{CP2,i+1} - L_{CP2,i}}{T_{CP2,i+1} - T_{CP2,i}} \tag{15}$$

where i is the index, $i \in \{1, 2, \ldots, n\}$, $L_{CP2,i}$ is the distance from the ith Type II CP to the stop bar, and $T_{CP2,i}$ is the timestamp of the i th Type II CP.

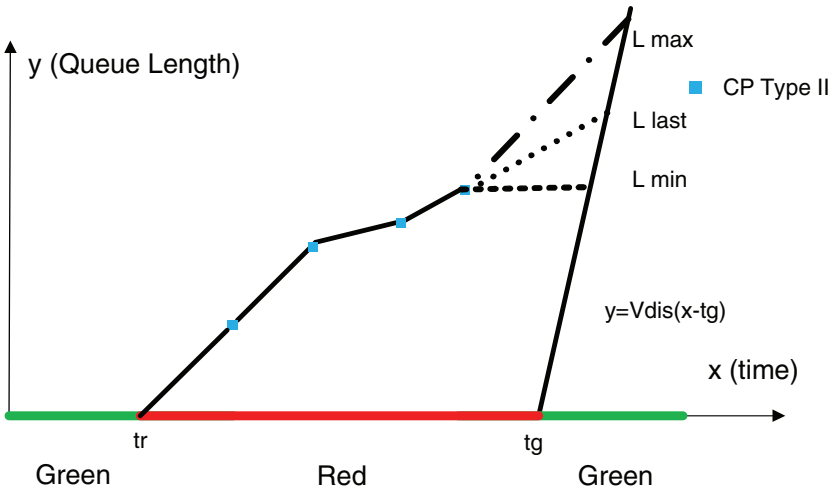

Figure 6 Queue formation under various arrival rates (color figure available online).

Therefore, several queue length estimates can be obtained using different arrival rates:

$$\begin{aligned} L_{\max} &= L_{CP2,n} + r_{\max} t_{\max} \\ L_{last} &= L_{CP2,n} + r_{n-1} t_{n-1} \\ L_{\min} &= L_{CP2,n} \end{aligned} \tag{16}$$

where $L_{\max}, L_{\min}, L_{last}$ are the three queue length estimates with the max queue increase rate, the last available queue increase rate, and no queue increase, respectively; $r_{\max} = \max(r_i)$, $t_{\max}, t_{last}$ are the time durations from the last Type II CP to the queue dissipation shockwave line using $q_{\max}$ or q_{n-1} (see Figure 6, and note that the line of the queue dissipation shockwave is: $y = v_{dis}(x - t_g)$).

Actually, $L_{\max}, L_{last}$ can be calculated in another way: They are the intersecting points of the queue dissipation shockwave with

$$y = r_{\max}(x - t_{CP2,n}) + L_{CP2,n} \tag{17}$$

and

$$y = r_{n-1}(x - t_{CP2,n}) + L_{CP2,n} \tag{18}$$

Therefore, $L_{\max}, L_{\min}$ can be calculated by the following:

$$L_{\max} = (L_{CP2,n} - r_{\max}(t_{CP2,n} - t_g)) \frac{v_{dis}}{v_{dis} - r_{\max}} \tag{19}$$

$$L_{last} = (L_{CP2,n} - r_{n-1}(t_{CP2,n} - t_g)) \frac{v_{dis}}{v_{dis} - r_{n-1}} \tag{20}$$

The queue length of the cycle can be estimated as a weighted average:

$$L_q = w_1 L_{\max} + w_2 L_{last} + w_3 L_{\min} \tag{21}$$

w_1, w_2, w_3 are the weights. $w_1 + w_2 + w_3 = 1; w_1, w_2, w_3 \in [0, 1]$. In the "Numerical Experiment" section, $w_1 = t_{g,n}/(t_{g,\max} + 2t_{g,n})$ and $w_2 = w_3$. $t_{g,n}$ is the time duration from the last Type II CP to the queue dissipation shockwave. Similarly, $t_{g,\max}$ is the time duration from the latter Type II CP of the segment with the max queue incremental rate to the queue dissipation shockwave line. They can be calculated as $t_g = \frac{L_{CP2}}{v_{dis}} + t_g - T_{CP2}$.

Note that the proposed models are based on the CPs on a single trajectory except for the queue length estimation under various arrival rates. Model improvement for various sample rates and sensitivity analysis of the sample rate are beyond the scope of this article.

NUMERICAL EXPERIMENT

Data Source

We used two types of data in the study. One is a simple two signalized intersection simulation network in Paramics and the other is a data set from NGSIM. In the simulation network, there is one exclusive through lane in the study direction, and the speed limit is 40 mph. The cycle length of the two intersections is 80 s with 45 s green. In the coordinated mode, the offset of the two signals is equal to the free-flow travel time between them. The demand flow rates have two levels: 800 veh/hr/ln for the nonpeak hour period and 1,800 veh/hr/ln for the peak hour period. The NGSIM data set used in this study is the trajectory data on the southbound link from 11th Street to 10th Street on Peachtree Street in Atlanta, Georgia. The data were collected between 4 PM and 4:15 PM on November 9, 2006. The signal was coordinated with a cycle length of 100 s.

Experiment Results

Signal Timing Detection

The signal detection error distributions are displayed in Figure 7 and 8, where the left y axis is the frequency and the right y axis is the percentage. Figure 7 shows the results of the isolated intersection case. Figure 8 shows the results of the coordinated intersection case. As discussed in the "Methodology" section, the detection of red uses one Type I CP each time and detection of green uses one Type III CP each time. All the available Type I and III CPs were used to compose the error distributions in Figure 7 and 8.

Figure 7 shows the results using 15 consecutive cycles' data for each of the two traffic demand levels. From nonpeak to peak period, the number of available samples increased from 150 to 500 approximately. For the isolated-intersection case, the detected start times of red and green are quite accurate. The detection of the start of green has better performance because the speed of the queue dissipation shockwave is nearly constant and the traffic in the queue discharging process usually has fewer disturbances. In contrast, the queue formation shockwave varies more and the traffic is "unstable far away" from the stop bar (Smilowitz, Daganzo, Cassidy, & Bertini, 1999, p. 225). For the peak hour case, errors distribute similarly to nonpeak hour except for some outliers. Further investigation reveals that these outliers were from the end of long queues (close to the upstream intersection) where the traffic is less stable and has more disturbances. It is sometimes observed that the shockwaves caused by signal were concealed by the local disturbances and even human eyes have difficulties in distinguishing them.

Figure 8 shows the results a coordinated intersection. Figure 8 (a) and (b) show the results using 15 consecutive cycles' data for each of the two traffic demand levels, where 90 samples were available in the nonpeak case and 158 were available in the peak hour case. Figure 8 (c) shows the results using 10 consecutive cycles' data by NGSIM, in which 88 samples were available. It is noteworthy that the signal timing cannot be detected if CPs are not available, (e.g., no vehicle is slowing down during a cycle).

The overall percentage error distribution is summarized in Figure 9. Approximately 50% errors for red detection are within

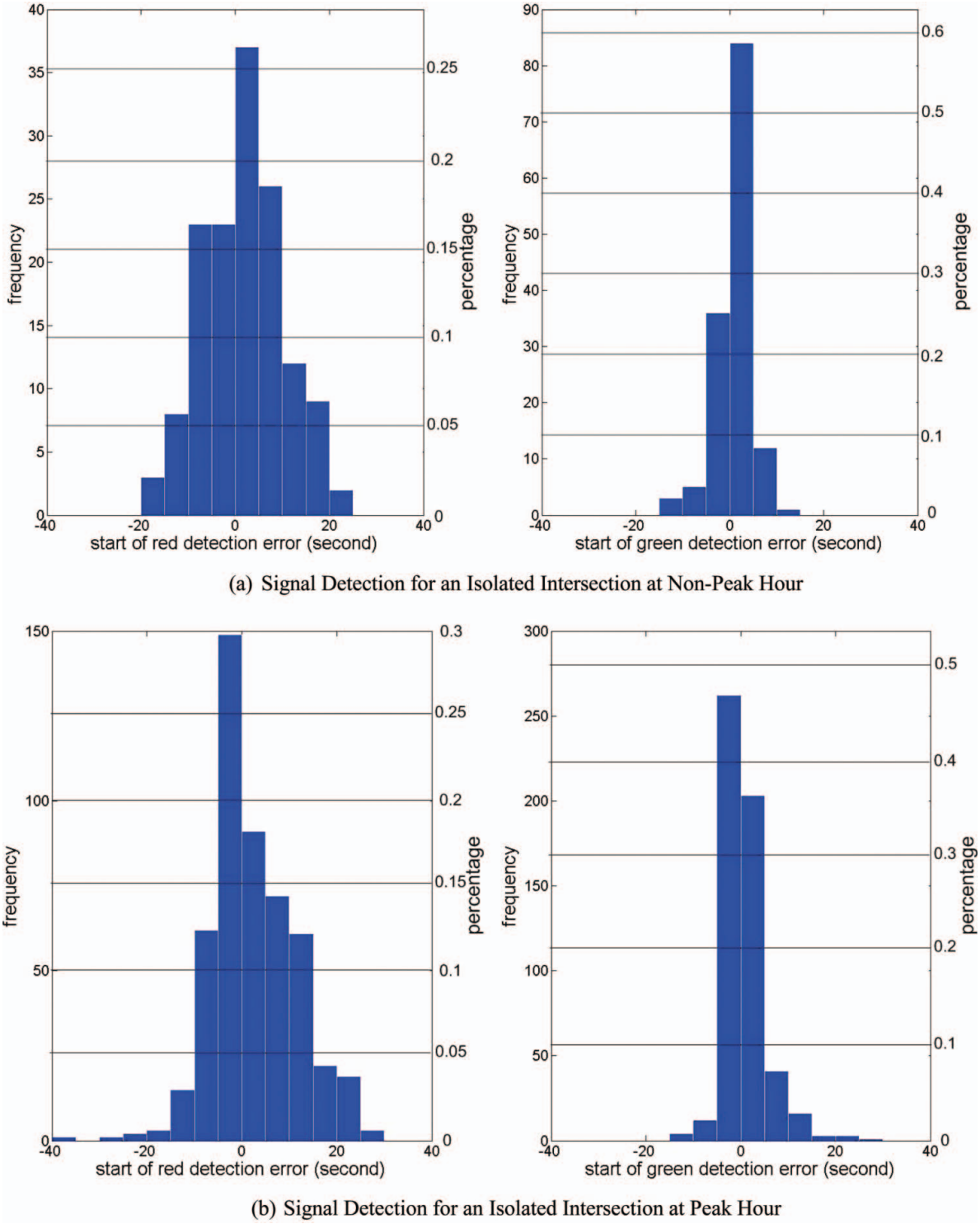

Figure 7 Signal detection for an isolated intersection (color figure available online).

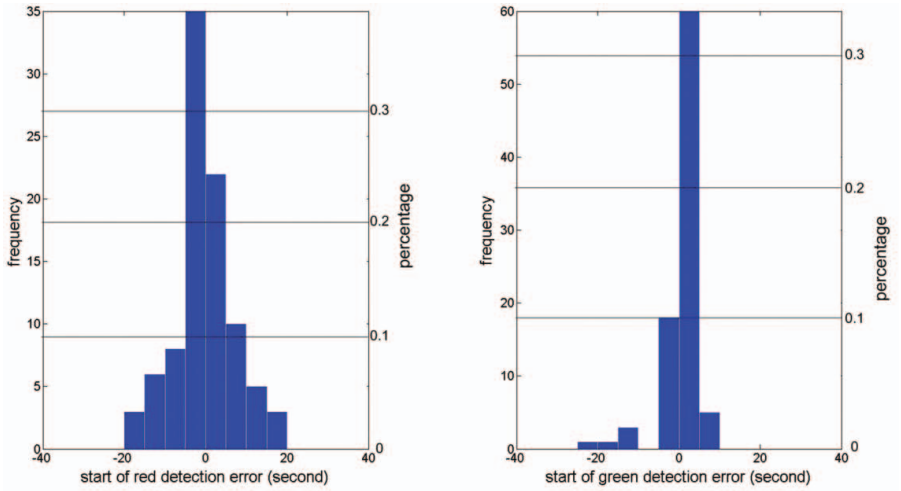

(a) Signal Detection for a Coordinated Intersection at Non-Peak Hour

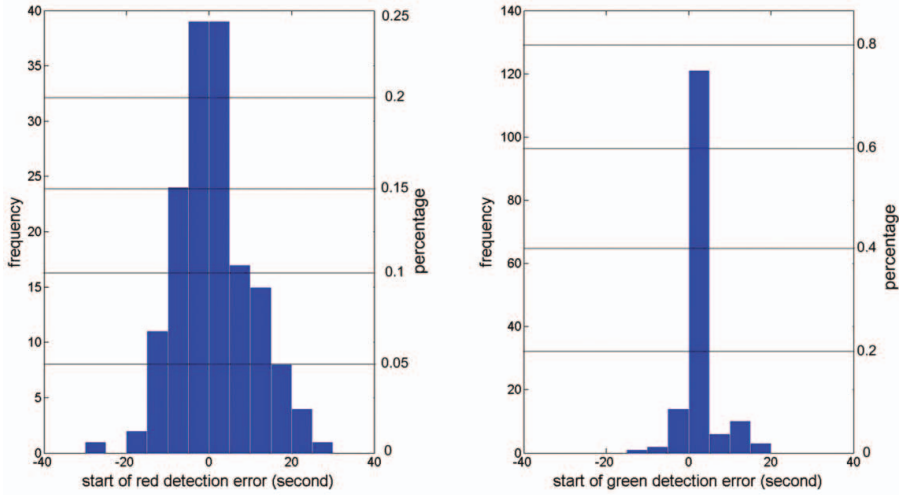

(b) Signal Detection for a Coordinated Intersection at Peak Hour

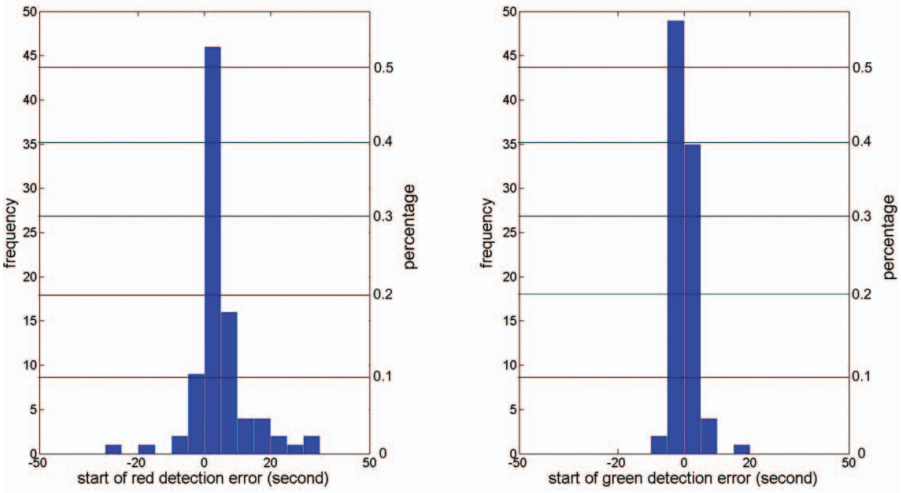

(c) Signal detection using NGSIM data

Figure 8 Detection of signal timing for a coordinated intersection (color figure available online).

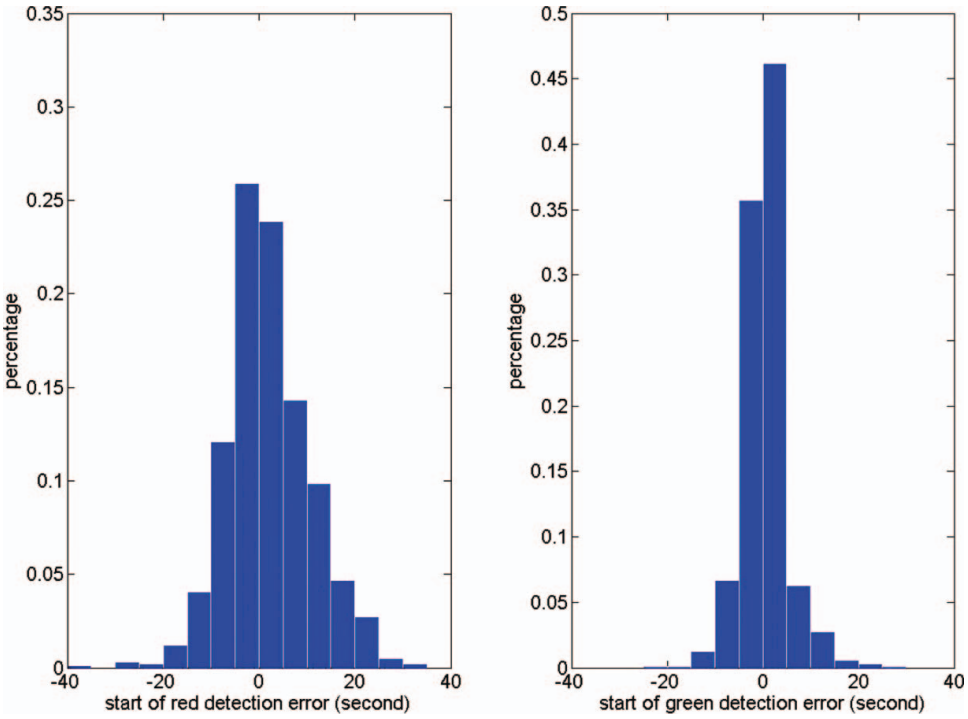

Figure 9 Summary of signal timing detection (color figure available online).

5 s and 80% are within 10 s. Approximately 90% errors for green detection are within 5 s. The results indicate a consistent and reliable signal detection performance.

Maximum Queue Length Estimation

The performance of the maximum queue length estimation is measured by the mean absolute percentage error (MAPE), which is calculated as follows:

$$MAPE = \frac{1}{n}\sum_{i=1}^{n}\left|\frac{Ground\ True - Estimation}{Ground\ True}\right| \times 100\% \tag{22}$$

where n is the total sample size.

The ground truth queue lengths were collected by observing the overall vehicle trajectories. For the isolated intersection cases, one trajectory was randomly selected for estimation in each cycle. For the coordinated intersection cases, three trajectories were randomly chosen in each cycle. For each case, the MAPE was calculated based on 20 independent runs to avoid randomness. The MAPEs for different scenarios are around 20% (Table 1).

Table 1 Mean absolute percentage error of queue length estimation.

		Number of cycles	Mean absolute percentage error
SIMU	Isolated (nonpeak)	12	18.41
	Isolated (peak)	12	19.56
	Coordinated (nonpeak)	12	22.43
	Coordinated (peak)	12	21.07
NGSIM	Lane 1*	7	23.35
	Lane 2**	7	24.16

*Lane next to median except left turn lane.
**Lane on the right.

Several possible causes contribute to the differences, including the errors in signal detection and end of queue detection, and more important, the variation of arrival rate within one cycle. The variation is so significant in the NGSIM dataset that in some cycles, arrival rate can change from nearly zero to close to capacity. Therefore, MAPEs are higher in the coordination scenarios than the ones for isolated intersections.

CONCLUSION AND FUTURE STUDY

This article describes an innovative approach for arterial intersection queue length estimation using vehicle trajectory data. The concept of CP connects the microscopic detections of individual trajectory with macroscopic performance measurement. The CP extraction algorithm has the potential for reducing communication cost for onboard GPS devices. Featuring all the major and minor turbulence and frictions of the vehicle, different types of CPs can be selected for a variety of applications. On the basis of the detected signal timing, the cycle-by-cycle queue length can be estimated for isolated and coordinated intersections. The model was evaluated under different signal and traffic demand conditions using simulated data and the NGSIM trajectory data.

Future studies should include (a) the improvement of the CP extraction algorithm and CP selection design to address the stop-and-go traffic, (b) the sensitivity analysis of the probe data error and sample rate for estimation performance and (c) the adoption of nonlinear shockwave models that are more suitable for arterial traffic flow and are able to support CP extraction and selection.

REFERENCES

Ahmed, H., El-Darieby, M., Abdulhai, B., & Morgan, Y. (2008). *Bluetooth and Wi-Fi-based mesh network platform for traffic monitoring*. Paper presented at the Transportation Research Board 87th Annual Meeting, Washington, DC, USA.

Alexiadis, V., Colyar, J., & Halkias, J. (2004). The Next Generation Simulation Program. *ITE Journal*, **74**(8), 22–26.

Balke, K. N., Charara, H., & Parker, R. (2005). *Development of a Traffic Signal Performance Measurement System (TSPMS)*. Texas Transportation Institute, College Station, TX, USA.

Ban, X., Herring, R., Hao, P., & Bayen, A. (2009). Delay pattern estimation for signalized intersections using sampled travel times. *Transportation Research Record: Journal of the Transportation Research Board*, **2130**, 109–119.

Berkow, M., Monsere, C. M., Koonce, P. J. V., Bertini, R. L., & Wolfe, M. (2009). *Prototype for data fusion using stationary and mobile data sources for improved arterial performance measurement*. Paper presented at the Transportation Research Board 88th Annual Meeting, Washington, DC, USA.

Cheu, R. L., Lee, D. H., & Xie, C. (2001). *An arterial speed estimation model fusing data from stationary and mobile sensors*. Paper presented at the Intelligent Transportation Systems, 2001. *2001 IEEE Intelligent Transportation Systems Conference Proceedings*, Oakland, CA, USA.

Claudel, C. G., Hofleitner, A., Mignerey, N., & Bayen, A. M. (2009). *Guaranteed bounds on highway travel times using probe and fixed data*. Paper presented at the Transportation Research Board 88th Annual Meeting, Washington, DC, USA.

Coifman, B. (2002). Estimating travel times and vehicle trajectories on freeways using dual loop detectors. *Transportation Research. Part A: Policy and Practice*, **36**, 351–364.

Comert, G., & Cetin, M. (2007). *Queue length estimation from probe vehicle location: Undersaturated conditions*. Paper presented at the Transportation Research Board 86th Annual Meeting, Washington, DC, USA.

Daganzo, C. F. (2005). A variational formulation of kinematic waves: Basic theory and complex boundary conditions. *Transportation Research Part B: Methodological*, **39**, 187–196.

Fontaine, M. D., & Smith, B. L. (2007). Investigation of the performance of wireless location technology-based traffic monitoring systems. *American Society of Civil Engineers: Journal of Transportation Engineering*, **133**, 157–165.

Geroliminis, N., & Skabardonis, A. (2005). Prediction of arrival profiles and queue lengths along signalized arterials by using a Markov decision process. *Transportation Research Record: Journal of the Transportation Research Board*, **1934**, 116–124.

Izadpanah, P., Hellinga, B., & Fu, L. (2009). *Automatic traffic shockwave identification using vehicles' trajectories*. Paper presented at the Transportation Research Board 88th Annual Meeting, Washington, DC, USA.

Lighthill, M. J., & Whitham, G. B. (1955a). On kinematic waves. I. Flood movement in long rivers. *Proceedings of the Royal Society of London. Series A, Mathematical and Physical Sciences*, **229**, 281–316.

Lighthill, M. J., & Whitham, G. B. (1955b). On kinematic waves. II. A theory of traffic flow on long crowded roads. *Proceedings of the Royal Society of London. Series A, Mathematical and Physical Sciences*, **229**, 317–345.

Liu, H. X., Ma, W., Wu, X., & Hu, H. (2008). *Development of a real-time arterial performance monitoring system using traffic data available from existing signal systems*. Minneapolis: University of Minnesota, Minnesota Department of Transportation.

Liu, H. X., Oh, J. S., Oh, S., Chu, L., & Recker, W. W. (2001). *Online traffic signal control scheme with real-time delay estimation technology*. Berkeley, CA: California Partners for Advanced Transit and Highways (PATH).

Lu, X., & Skabardonis, A. (2007). *Freeway traffic shockwave analysis: Exploring NGSIM trajectory data*. Paper presented at the Transportation Research Board 86th Annual Meeting, Washington, DC, USA.

National Transportation Operations Coalition. (2007). *2007 National Traffic Signal Report Card Technical Report*. Washington, DC: Institute of Transportation Engineers.

Newell, G. F. (1993). A simplified theory of kinematic waves in highway traffic, Part I: General theory. *Transportation Research. Part B: Methodological*, **27**, 281–287.

Pan, C., Lu, J., Wang, D., & Ran, B. (2007). Data collection based on Global Positioning System for travel time and delay for arterial roadway network. *Transportation Research Record: Journal of the Transportation Research Board*, **2024**, 35–43.

Qiu, Z., & Ran, B. (2008). *Kalman filtering applied to network-based cellular probe traffic monitoring*. Paper presented at the Transportation Research Board 87th Annual Meeting, Washington, DC, USA.

Richards, P. I. (1956). Shock waves on the highway. *Operations Research*, **4**(1), 42–51.

Ritchie, S. G., Jeng, S.-T., Tok, Y. C., & Park, S. (2008). *Corridor deployment and investigation of anonymous vehicle tracking for real-time traffic performance measurement*. Berkeley, CA: California Partners for Advanced Transit and Highways (PATH).

Robinson, S., & Polak, J. W. (2005). Modeling urban link travel time with inductive loop detector data by using the k-NN method. *Transportation Research Record: Journal of the Transportation Research Board*, **1935**, 47–56.

Skabardonis, A., & Geroliminis, N. (2008). Real-time monitoring and control on signalized arterials. *Journal of Intelligent Transportation Systems*, **12**(2), 64–74.

Smilowitz, K. R., Daganzo, C. F., Cassidy, M. J., & Bertini, R. L. (1999). Some observations of highway traffic in long queues. *Transportation Research Record*, **1678**, 225–233.

Turner, S. M., Eisele, W. L., Benz, R. J., & Holdener, D. J. (1998). *Travel time data collection handbook*. Texas Transportation Institute, Federal Highway Administration.

Viti, F., & van Zuylen, H. J. (2009). The dynamics and the uncertainty of queues at fixed and actuated controls: A probabilistic approach. *Journal of Intelligent Transportation Systems*, **13**(1), 39–51.

Wilson, R. E. (2008). *From inductance loops to vehicle trajectories*. Paper presented at the Symposium on the Fundamental Diagram: 75 Years (Greenshields 75 Symposium), Woods Hole, MA, USA.